# Reduced release probability prevents vesicle depletion and transmission failure at dynamin mutant synapses

Xuelin Lou[a,b,1], Fan Fan[a,b], Mirko Messa[a], Andrea Raimondi[a,2], Yumei Wu[a], Loren L. Looger[c], Shawn M. Ferguson[a], and Pietro De Camilli[a,1]

[a]Department of Cell Biology, Howard Hughes Medical Institute, Program in Cellular Neuroscience, Neurodegeneration and Repair, Kavli Institute for Neuroscience, Yale University School of Medicine, New Haven, CT 06510; [b]Department of Neuroscience, School of Medicine and Public Health, University of Wisconsin, Madison, WI 53706; and [c]Howard Hughes Medical Institute, Janelia Farm Research Campus, Ashburn, VA 20147

Contributed by Pietro De Camilli, January 4, 2012 (sent for review November 19, 2011)

**Endocytic recycling of synaptic vesicles after exocytosis is critical for nervous system function. At synapses of cultured neurons that lack the two "neuronal" dynamins, dynamin 1 and 3, smaller excitatory postsynaptic currents are observed due to an impairment of the fission reaction of endocytosis that results in an accumulation of arrested clathrin-coated pits and a greatly reduced synaptic vesicle number. Surprisingly, despite a smaller readily releasable vesicle pool and fewer docked vesicles, a strong facilitation, which correlated with lower vesicle release probability, was observed upon action potential stimulation at such synapses. Furthermore, although network activity in mutant cultures was lower, $Ca^{2+}$/calmodulin-dependent protein kinase II (CaMKII) activity was unexpectedly increased, consistent with the previous report of an enhanced state of synapsin 1 phosphorylation at CaMKII-dependent sites in such neurons. These changes were partially reversed by overnight silencing of synaptic activity with tetrodotoxin, a treatment that allows progression of arrested endocytic pits to synaptic vesicles. Facilitation was also counteracted by CaMKII inhibition. These findings reveal a mechanism aimed at preventing synaptic transmission failure due to vesicle depletion when recycling vesicle traffic is backed up by a defect in dynamin-dependent endocytosis and provide new insight into the coupling between endocytosis and exocytosis.**

active zone | short-term synaptic plasticity | syndapin | membrane fission

Synapses undergo several forms of short-term plasticity with timescales ranging from tens of milliseconds to several minutes (1, 2). The interplay of multiple forms of short-term plasticity, including facilitation and depression, leads to bidirectional changes of synaptic strength. Whereas both pre- and postsynaptic factors contribute to synaptic plasticity, short-term plasticity is due primarily to regulatory mechanisms occurring in the presynaptic compartment. Synaptic vesicle availability and release probability play important roles in this process (1, 3–5). Because of the limited number of vesicles in the readily releasable pool (RRP), the availability of synaptic vesicles for exocytosis rapidly becomes the limiting step during high-frequency action potential firing, leading to synaptic depression (1, 4–6). Recovery from synaptic depression relies upon the replenishment of the RRP (7, 8), a process that is at least partially dependent on the endocytic recycling of synaptic vesicle membranes (9, 10).

During a brief stimulation, synapses do not rely on endocytosis to support secretion because of the existence of reserve pools of vesicles in addition to the RRP. In contrast, during sustained action potential firing, endocytosis-dependent vesicle reformation becomes essential for continuous synaptic transmission (11–14). For example, in model organisms, genetic or biochemical perturbations of synaptic vesicle endocytosis have typically minimal effects on the initial synaptic transmission, although they strongly impact the release of neurotransmitter in response to prolonged stimulatory trains (15–26).

Recent studies also suggest that a feedback between endocytosis and exocytosis may occur over very short timescales (milliseconds to seconds) (1, 7, 27, 28). For example, the efficient clearing of fusion sites via endocytosis may affect availability of vesicle fusion sites for transmitter release. Proteins with a dual role in exo- and endocytosis have been identified (such as synaptotagmin, synaptobrevin, and endophilin) (29–34), and signaling pathways that produce interrelated effects on exo- and endocytosis have been described (28).

A protein that plays a key role in endocytic membrane recycling at synapses is the GTPase dynamin (9, 22, 35–38). Dynamin assembles around the necks of endocytic pits and participates in their fission via a GTP-hydrolysis–dependent conformational change leading to their constriction (36, 39–46). Three *dynamin* genes are present in mammals, which encode dynamin 1, 2, and 3, respectively. Dynamin 2, which is ubiquitously expressed, has a housekeeping endocytic function in all cells (47). Dynamin 1 and 3 are expressed primarily in neurons, where they are concentrated in nerve terminals and account for the majority of the total neuronal dynamin, with dynamin 1 being by far the predominant species (9, 48, 49). In recent gene knockout (KO) studies in mice, we have found that whereas both dynamin 1 and dynamin 3 are concentrated in nerve terminals, neither isoform is essential for synaptic vesicle recycling (9, 35). A main role of dynamin 1 is to allow synapses to scale up the speed of endocytosis when strong and prolonged stimuli result in massive exocytosis (38). This function is likely to be dependent, at least in part, on its very high level of expression. The absence of dynamin 3 alone has little impact on synaptic function, but worsens the presynaptic defect produced by the lack of dynamin 1 (35).

In neuronal cultures derived from dynamin 1 and 3 double-KO (DKO) mice, synaptic vesicles are greatly reduced in number and much of the synaptic vesicle membrane material is sequestered in clathrin-coated pits. Accordingly, as we have shown, excitatory postsynaptic currents (EPSCs) are severely decreased in size at such synapses. However, the impact of the lack of two neuronal dynamins (dynamin 1 and 3) on the efficiency of neurotransmitter release in response to continuous action potential firing and on the synaptic plasticity has not been investigated. Given the profound impact of synaptic plasticity on neuronal communication and on information processing in neural circuits, we have now further analyzed such an impact.

Author contributions: X.L. and P.D.C. designed research; X.L., F.F., M.M., A.R., Y.W., and S.M.F. performed research; L.L.L. contributed new reagents/analytic tools; X.L., F.F., M.M., A.R., Y.W., and S.M.F. analyzed data; and X.L., S.M.F., and P.D.C. wrote the paper.

The authors declare no conflict of interest.

Freely available online through the PNAS open access option.

[1]To whom correspondence may be addressed. E-mail: Pietro.decamilli@yale.edu or xlou3@wisc.edu.

[2]Present address: Department of Neuroscience and Brain Technologies, Istituto Italiano di Tecnologia, via Morego, 30 16163 Genoa, Italy.

See Author Summary on page 2711 (volume 109, number 8).

This article contains supporting information online at www.pnas.org/lookup/suppl/doi:10.1073/pnas.1121626109/-/DCSupplemental.

## Results

**Decreased but Still Synchronized Synaptic Network Activity in the Absence of Dynamin 1 and 3.** We have shown previously that although DKO mice for both dynamin 1 and 3 die perinatally, brain cells derived from newborn DKO mice differentiate in vitro and form synaptic networks that are morphologically similar to those of control mice (35). A preliminary analysis of synaptic activity in these cultures revealed slightly reduced frequency of miniature excitatory postsynaptic currents (mEPSCs) and a severe reduction of evoked EPSCs (35).

We have now compared overall neuronal network activity in cultures from control and DKO mouse brains, using ratio-metric $Ca^{2+}$ imaging (Fig. 1). Two types of $Ca^{2+}$ signals were observed in individual cells: fast $Ca^{2+}$ spikes and slow $Ca^{2+}$ waves with large amplitude, arising from neurons and surrounding glia cells, respectively (Fig. S1). Fast $Ca^{2+}$ spikes can be selectively blocked by 1 μM tetrodotoxin (TTX), indicating occurrence of action potential firing in neurons (Fig. S1*A*) (50, 51). The number and amplitude of these spikes were further drastically enhanced by administration of high extracellular $K^+$ solution, a global stimulus of neuron depolarization, and synaptic transmission (Fig. S1*B*). The slow $Ca^{2+}$ waves were insensitive to both TTX and high $K^+$ (Fig. S1 *A* and *B*).

The abundance of fast, in many cases synchronous, spikes in control cultures (Fig. 1 *A* and *C*) demonstrated the occurrence of vigorous synaptic transmission and often synchronized network activity (51). In DKO cultures (Fig. 1 *B* and *D*), fast spikes occurred at much lower frequency, but with similar amplitude (Fig. 1 *E* and *F*). However, in these cultures as well there were examples of synchronous events, reflecting network activity mediated by synaptic transmission (Fig. 1*D*). A small population of neurons did not show obvious $Ca^{2+}$ spikes in either culture and this population was greater in DKO (31% of all of the tested neurons) than in controls (19% of neurons tested). Basal $Ca^{2+}$ levels were very slightly higher in DKO neurons (Fig. 1*G*). Furthermore, the lack of dynamin 1 and 3 had little effect on the slow $Ca^{2+}$ waves of glial cells (Fig. S1*C*).

These data demonstrate that absence of dynamin 1 and 3 dramatically scales down, but does not abolish, the network activity in these neuronal circuits, consistent with residual synaptic vesicle recycling function in DKO neurons.

**Strong Synaptic Facilitation at Dynamin 1 and 3 DKO Synapses.** DKO synapses have a lower content of synaptic vesicles and, accordingly, smaller evoked EPSCs (35). Here we examined short-term plasticity changes at excitatory DKO synapses, using whole-cell patch clamp recordings. According to the vesicle pool depletion hypothesis (2, 4), one would expect enhanced synaptic depression and faster vesicle pool depletion during continuous stimulation in DKO synapses. To our surprise, we detected strong facilitation, which is in strong contrast to the enhanced synaptic depression observed at synapses of mice (16, 17, 52), *Caenorhabditis elegans* (20), and *Drosophila* (10, 15, 21, 53) harboring inactivating mutations of endocytic proteins. We conclude that the impact of the lack of dynamin 1 and 3 on exo–endocytosis coupling at active zones, and thus on short-term plasticity, is different from that of other perturbations that affect the endocytic recycling of synaptic vesicles.

EPSCs evoked by a train of 30 action potentials (APs) at 1 Hz in a control and a DKO neuron are shown in Fig. 2 *A* and *B*, respectively. The first EPSC was much smaller in DKO neurons (Fig. 2*A*), as expected (35). However, in contrast to the depression observed at the control neuron, a strong facilitation was observed at the DKO neuron. Such facilitation during the

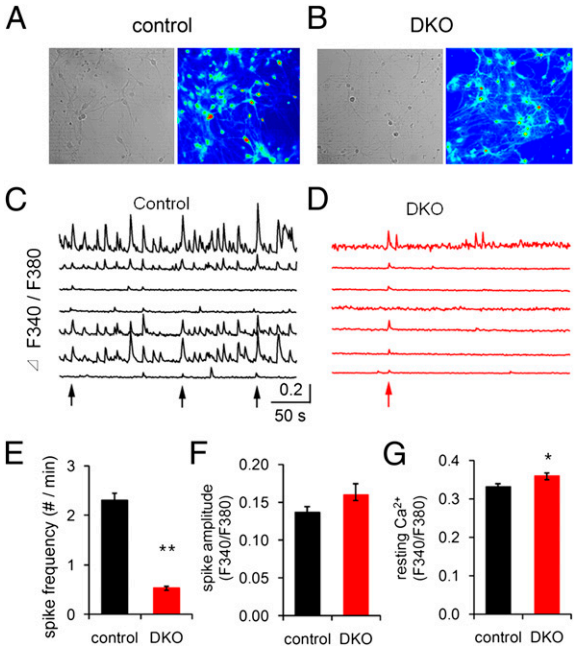


**Fig. 1.** Reduced spontaneous network activity in cortical neuronal cultures derived from dynamin 1 and 3 double-KO (DKO) mice. (*A* and *B*) Differential interference contrast images and fluorescence images excited at 380 nm (F380) from a control (*A*) and a DKO (*B*) culture preloaded with Fura-2 AM under a 20× water immersion objective (NA = 0.6). (*C* and *D*) Intracellular $Ca^{2+}$ responses (F340/F380 fluorescence) of individual neurons from control and DKO cultures shown in *A* and *B*. Arrows indicate synchronized $Ca^{2+}$ spikes. (*E*–*G*) $Ca^{2+}$ spike frequency (*E*), amplitude (*F*), and resting $Ca^{2+}$ levels (*G*) in control and DKO cultures (control, $n = 99$ neurons; DKO, $n = 85$ DKO neurons; $*P < 0.05$, $**P < 0.01$).

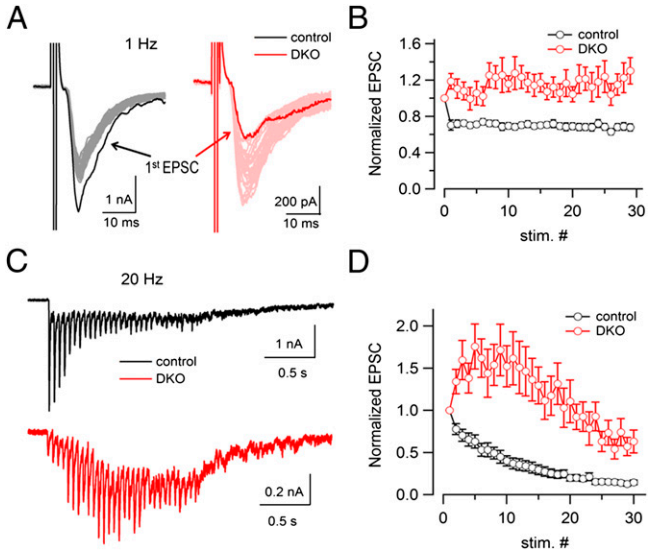


**Fig. 2.** Strong synaptic facilitation in response to both low- and high-frequency stimulation at DKO synapses. (*A*) Superimposed traces of EPSCs elicited by 30 APs at 1 Hz in a control and a DKO neuron. The first EPSC is shown as a solid trace. Note the different EPSC scales for the neurons of the two genotypes. (*B*) Average normalized EPSCs elicited by 30 APs at 1 Hz from control ($n = 21$) and DKO neurons ($n = 18$). EPSCs were normalized to the peak amplitude of the first EPSC in each AP train. (*C*) EPSCs recorded from a control and a DKO neuron in response to 30 APs at 20 Hz. (*D*) Average normalized EPSCs elicited by 30 APs at 20 Hz from control ($n = 18$) and DKO ($n = 16$) neurons. EPSCs were normalized to the peak amplitude of the first EPSC in each AP train. Note the depression at control synapses and facilitation at DKO synapses.

30-APs (at 1 Hz) stimulation was consistently observed, as demonstrated in Fig. 2*B* where the average EPSC values from different recordings were normalized to the first EPSC peak amplitude. The synaptic facilitation was even stronger when the same number of APs was delivered at higher frequency (20 Hz) (see Fig. 2*C* for a representative control and DKO synapses and Fig. 2*D* for the average responses). The transient enhancement of the EPSCs at both frequencies was followed by depression, likely reflecting a gradual depletion of the RRP of vesicles. However, the normalized DKO curve never crossed the control curve despite the smaller RRP, indicating persistence of facilitation throughout the stimulatory train.

A similar persistent facilitation was also observed after a prolonged high-frequency stimulus (300 APs at 10 Hz; Fig. 3 *A*–*C*). Fig. 3*A* shows individual EPSCs from a control and a DKO neuron recorded at different time points during such stimulus. The time courses of average EPSCs (Fig. 3*B*) as well as their normalized values (normalized to the size of the first EPSC) (Fig. 3*C*) demonstrate that only a few quantal events were detectable at the end of the stimulation in both control and DKO neurons, likely reflecting dramatic vesicle depletion. However, in contrast to the fast depression observed in control synapses, DKO synapses showed an initial strong facilitation (note in Fig. 3*A* that the 10th EPSC was approximately twofold bigger than the initial EPSC), which was followed by a slow depression. Because of the strong facilitation in DKO synapses, the normalized EPSC curves from control and DKO synapses clearly separated at the beginning of the stimulation and then tended to merge at the end of stimulation, but again without crossing each other before the RRP is close to the depletion state (Fig. 3 *B* and *C*). These results demonstrate reluctance to vesicle depletion at DKO synapses.

We next examined the time course of synaptic transmission recovery as tested by APs delivered at 0.2 Hz, starting immediately after the end of the 300-AP/10-Hz stimuli. As shown by the analysis of individual EPSCs (Fig. 3*D*) and by curves reporting either absolute EPSC amplitude (Fig. 3*E*) or normalized EPSC (relative to its prestimulus value) (Fig. 3*F*), EPSCs recovered up to ~75% of the prestimulus amplitude in 5 min in control cultures, with a biphasic time course (fast and slow time constants of 8.5 s and 150 s, respectively). In contrast, only the fast recovery (time constant of 7.5 s) was observed in DKO cultures, followed with a steady state at ~50% of the prestimulus amplitude.

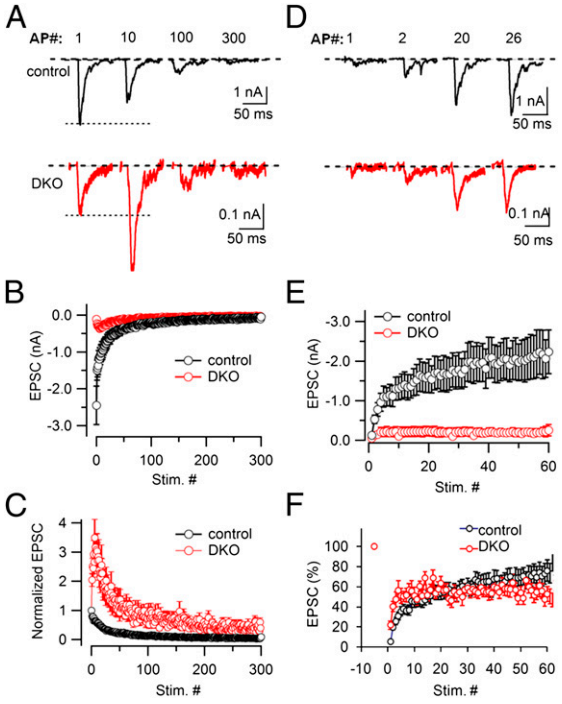


**Fig. 3.** Synaptic vesicle depletion and recovery in the absence of dynamin 1 and 3. (*A*) Individual EPSCs recorded during a 300-APs train at 10 Hz (i.e., a stimulus leading to a near depletion of releasable synaptic vesicles) in a control and a DKO neuron. The AP number is indicated at the top. (*B* and *C*) Average EPSC amplitudes (*B*) and normalized EPSCs (*C*) from control ($n = 14$) and DKO neurons ($n = 14$). (*D*) Recovery of synaptic transmission immediately after the vesicle depletion induced by 300 APs at 10 Hz in a control neuron and a DKO neuron. Recovery was estimated by EPSCs induced with AP stimulation at 0.2 Hz. Individual EPSCs were recorded at different times during the recovery. The AP number is indicated at the top. (*E* and *F*) Time course of EPSC recovery after vesicle depletion in control ($n = 12$) and DKO neurons ($n = 15$). EPSCs were normalized to the first EPSC amplitude of the depletion train (*F*).

**No Major Postsynaptic Contribution to the Observed Synaptic Facilitation.** Short-term synaptic plasticity can have presynaptic and postsynaptic origins (1, 2, 4). The traffic of α-amino acid-3-hydroxy-5-methyl-4-isoxazole (AMPA) receptors (AMPARs) in dendritic spines undergoes activity-dependent changes (54), and these events are believed to underlie long-term plasticity and memory. Because dynamin-dependent AMPAR endocytosis is thought to control the levels of a pool of mobile surface-exposed AMPARs (55–58), a postsynaptic contribution to the facilitation observed at DKO synapses should be considered. We investigated therefore whether dynamin function may modulate synaptic strength in spines by disrupting the AMPAR trafficking.

The relative ratio of synaptic currents through AMPARs and N-methyl-D-aspartate (NMDA) receptors at individual synapses has been widely used to study postsynaptic AMPA trafficking, because levels of surface exposed NMDA receptors are relative stable (59). Thus, if fast AMPAR trafficking contributes significantly to the facilitation at DKO synapses, a change of AMPA/NMDA ratio is expected. Fig. 4*A* shows AMPA and NMDA currents recorded at a control and a DKO neuron. Because the kinetics of AMPA and NMDA current differ dramatically, they can be clearly separated temporally without using specific pharmacological blockers (60, 61). NMDA current amplitudes were extracted at 100 ms (+60 mV) after stimulation, a time point at which the AMPA current had completely decayed (61). Although both AMPA and NMDA currents were much smaller at DKO than at control synapses (Fig. 4 *A* and *B*), no significant difference was observed in the ratio of AMPA/NMDA currents between the two groups (Fig. 4 *B* and *C*). These data suggest that postsynaptic mechanisms contribute little, if at all, to the changes of short-term plasticity observed at DKO synapses.

Another possibility is that some silent synapses could be activated after the first AP by the fast recruiting of AMPA receptors to previously silent synapses, thus contributing to the subsequent synaptic enhancement. However, the very fast timescale of facilitation (it occurs within subseconds after the first AP) seems incompatible with the timescale of AMPAR trafficking (seconds to minutes). This possibility was further tested by comparing the paired-pulse ratio (PPR) of AMPA and NMDA currents (61) after two closely spaced stimuli. Upon a paired-pulse (2 APs with 100-ms interval) stimulation at individual DKO synapses, the PPR was similar for AMPA currents and for NMDA currents (Fig. 4*D*), speaking against a role of quick activation of silent synapses in the facilitation observed at DKO synapses. We conclude that postsynaptic mechanisms do not play a major role in the synaptic facilitation produced by the lack of dynamin 1 and 3.

**Decreased Readily Releasable Vesicle Pool Size and Synaptic Release Probability.** We next used two different approaches to determine the changes of RRP and release probability at DKO synapses. First, we used stimulation by acute high osmolarity (62). Upon locally puffing 500 mM sucrose for 5 s onto the recorded neuron,

a large, slow inward current, which reflects glutamate release from the surrounding synapses, was observed in control neurons (Fig. 5 *A* and *B*). The response to this stimulus was less robust at DKO synapses (~50% decrease in peak amplitude and 70% decrease in total charge transfer on average) (Fig. 5*B*), and this difference was smaller than the reduction in the amplitude of AP-evoked EPSCs (~90%) (Fig. 2 *A* and *C*). Paired stimuli of hypertonic sucrose further revealed a decreased refilling rate of the RRP at DKO synapses (Fig. S2), most likely reflecting the strongly reduced vesicle number within terminals.

Second, we estimated RRP size within these synapses using a train of APs (30 APs, 20 Hz, Fig. 5 $C_1$–$D_3$) in high extracellular $Ca^{2+}$ (10 mM) (63, 64). The high $Ca^{2+}$ condition maximizes the release probability and minimizes the submaximum transmitter release during the stimulation (65); whereas this condition leads to faster depression than at physiological $Ca^{2+}$ concentration (2 mM), the kinetics of depression were still much slower at DKO synapses relative to controls (Fig. 5$C_2$), demonstrating a reluctance of DKO synapse to deplete the RRP vesicles. The RRP size, derived from linear back extrapolation of the cumulative peak EPSCs to time 0 (Fig. 5$C_3$), is strongly decreased at DKO synapses (Fig. 5$D_2$).

On the basis of the EPSC size triggered by the first AP (Fig. 5$D_1$) and the corresponding RRP size at individual synapses (Fig. 5$D_2$), we found that DKO synapses had a significantly lower release probability (defined by the ratio between EPSC amplitude and RRP size) than control synapses (Fig. 5$D_3$). Of note, the size of the RRP estimated by sucrose (Fig. 5 *A* and *B*) was bigger than the one estimated by action potential stimulation (Fig. 5$D_2$), indicating that RRP vesicles at DKO synapses are less responsive to physiological stimulation (APs) and are reluctant to undergo exocytosis in response to this stimulus.

Release probability was further analyzed with a paired-pulses test with variable interpulse intervals between the two APs. In contrast to the synaptic depression at control synapses, DKO synapses showed significant facilitation at most of the time intervals tested (Fig. 5*E*), so that the curve of paired-pulse ratios was up-shifted for DKO synapses relative to control synapses (Fig. 5*F*). These data supports a significant decrease of release probability in DKO synapses compared with controls.

One of the key factors affecting release probability is $Ca^{2+}$ influx. To determine potential differences in $Ca^{2+}$ influx between DKO and control synapses, we used the fluorescence of SyGCaMP3, a fusion protein compromising the high-affinity, genetically encoded $Ca^{2+}$ probe GCaMP3 (66) and synaptophysin for selective presynaptic targeting. A similar method using SyGCaMP2 was recently applied to monitor synaptic $Ca^{2+}$ signals (67, 68). No significant differences of the SyGCaMP3 signals were observed in our experiments between control and DKO synapses (Fig. S3), which speaks against a major impact of the lack of dynamin 1 and dynamin 3 on $Ca^{2+}$ dynamics, although potential effects of an abnormal localization of SyGCaMP3 in DKO nerve terminals cannot be ruled out.

Collectively, these findings demonstrate that the two neuronal dynamins are needed to maintain a normal RRP of vesicles and that in their absence a lower release probability counteracts the rapid depletion of this pool.

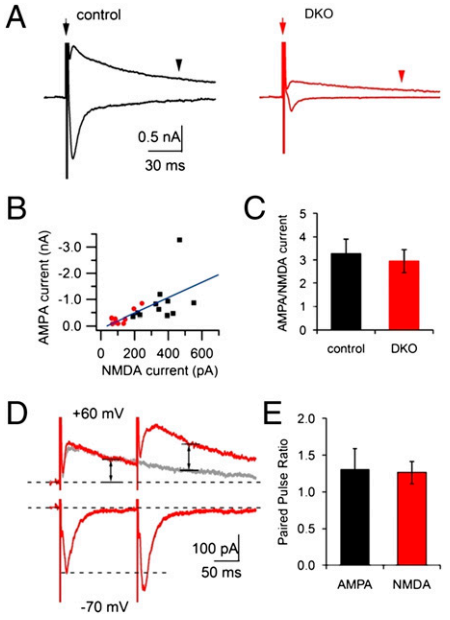


**Fig. 4.** Presynaptic origin of the facilitation observed at DKO synapses. (*A*) AMPA and NMDA currents triggered by single APs. The amplitude of NMDA currents recorded at +60 mV (holding potential) was measured at a time point of 100 ms (arrowhead) after the AP stimulation (arrow), the same as for *B*–*D*. (*B* and *C*) Smaller AMPA and NMDA current amplitude (*B*) but similar AMPA/NMDA current ratio (*C*) at control ($n$ = 11) and DKO neurons ($n$ = 9). (*D*) AMPA and NMDA currents induced by a paired pulse (at 100-ms intervals). The second NMDA current amplitude (second arrow) was measured at 100 ms after the second AP but subtracting the residual component of NMDA current from the first AP (gray trace, obtained by a single AP at the same neuron). (*E*) Paired-pulse ratio of AMPA/NMDA currents in both control and DKO cultures ($n$ = 5 for each).

**Facilitation at DKO Synapses Is Activity Dependent and Reversible.** We showed previously that TTX treatment largely reverses at least some of the structural and biochemical changes produced by the lack of the neuronal dynamins, i.e., the massive increase in clathrin-coated pits, the accompanying decrease of the number of synaptic vesicles, and the increase in the phosphorylation state of synapsin 1 at $Ca^{2+}$/calmodulin-dependent protein kinases II (CaMKII) dependent sites (sites 2 and 3) and its dispersed distribution (9, 35). We have now examined whether TTX also reverses electrophysiological parameters. As shown in Fig. 6*A*, following an overnight incubation of the neuronal cultures with 1 μM TTX, the EPSC amplitude increased in both control and DKO synapses, in agreement with the homeostatic up-regulation of synaptic strength known to be produced by such treatment (69). Importantly, however, the relative increase of average EPSC amplitude was stronger at DKO synapses (327 ± 92.8% of untreated control, $n$ = 10) than at control synapses (139 ± 21.7%, $n$ = 14, $P < 0.05$), although it remained lower than in controls (Fig. 6*A*, *Right*). Strikingly, in DKO synapses under these conditions, low-frequency AP stimulation elicited synaptic depression similar to that in controls, rather than facilitation, despite its much smaller initial EPSC (Fig. 6*B*). Upon high-frequency stimulation, synaptic facilitation also disappeared and converted to depression, but such depression remained much weaker than at control synapses (Fig. 6*C*). The reversal of facilitation following TTX treatment speaks against the possibility that the change of short-term plasticity observed in DKO neurons may result from chronic developmental or other long-term compensatory changes.

We next used electron microscopy to determine whether the reversibility of the electrophysiological changes upon TTX treatment correlated with reversible changes in the number of synaptic vesicles docked at active zones, i.e., the vesicles that are thought to represent the RRP. In DKO nerve terminals, not only was the synaptic vesicle cluster smaller than in controls (35), but also the numbers both of vesicles within 1 μm of the active zones and of the docked vesicles were fewer (Fig. 7 *A* and *B*), in agreement with the smaller RRP detected by electrophysiological recordings. Notably, TTX treatment resulted in an increase in the number of docked vesicles both at control and DKO synapses (Fig. 7*C*), but this increase was much more robust at DKO

synapses (Fig. 7*D*), where a partial recovery of the global number of synaptic vesicles was also observed (35). Although after TTX treatment the number of docked vesicles at active zones of DKO synapses was restored to the level of TTX-untreated control synapses (Fig. 7*C*), the EPSC amplitude was still smaller (<50% of control), indicating that additional mechanisms, besides vesicle availability, affect the probability of release at DKO synapses.

**Increased CaMKII Activity Contributes to Synaptic Facilitation at DKO Synapses.** We explored biochemical changes at DKO synapses that could provide insight into mechanisms underlying synaptic facilitation. As we have reported previously (35), a markedly increased phosphorylation state of synapsin 1 at sites 2 and 3, i.e., the $Ca^{2+}$-dependent (CaMKII) regulated sites (70, 71), occurs in DKO cultures under conditions of spontaneous network activity. To determine whether this change reflects an increased activity state of CaMKII, despite the lower activity state of synapses, we have now assessed by immunoblotting the phosphorylation of βCaMKII at threonine 286, a site that undergoes autophosphorylation leading to autoactivation. As shown in Fig. 8*A*, an increase of the signal in DKO cultures relative to controls was observed, although the total CaMKII level (as revealed by a pan-CaMKII antibody) was the same in DKO and controls (Fig. 8*A*).

These findings raise the possibility that the increased activity state of CaMKII could contribute to the short-term plasticity observed at DKO synapses. We tested this possibility by performing experiments in the presence of Ant-AIP-II, a cell-permeable version (due to a fusion to the *Antennapedia* transport peptide) of the autocamtide-2 related inhibitory peptide II (AIP-II), a specific, noncompetitive CaMKII inhibitor. Ant-AIP-II has a potent inhibitory effect on CaMKII activity when added to the extracellular medium of living neurons (72, 73). Accordingly, as shown in Fig. 8*B*, addition of Ant-AIP-II to control cultures reduced the phosphorylation of threonine 286 in CaMKII and of

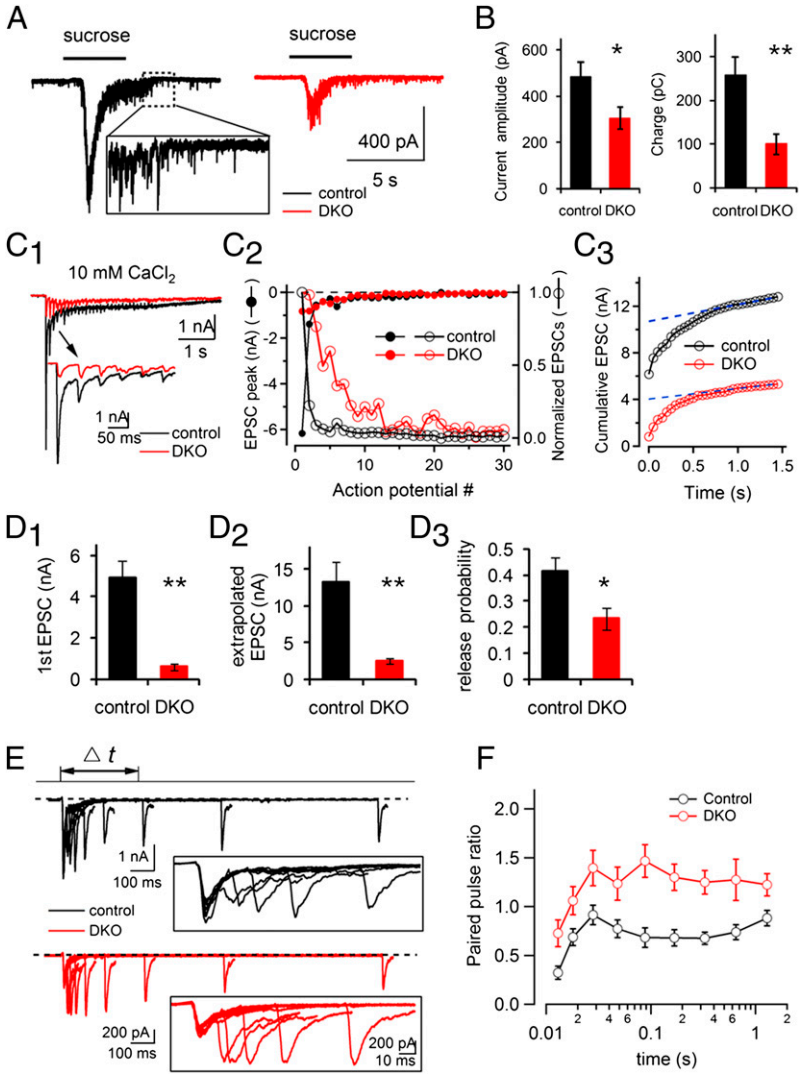


**Fig. 5.** Readily releasable pool (RRP) and vesicle release probability are reduced in DKO synapses. (*A*) A total of 500 mM sucrose evoked EPSCs from a control and a DKO neuron. (*B*) The RRP, as estimated by both EPSC amplitude and total charge transfer, is smaller in DKO synapses than in control ($n$ = 21, control; $n$ = 18, DKO; $^*P < 0.05$, $^{**}P < 0.01$). ($C_1$–$C_3$) Estimation of the RRP by a high-frequency AP train in 10 mM extracellular $CaCl_2$. ($C_1$) EPSCs evoked by 30 APs at 20 Hz. ($C_2$) EPSC peaks (solid circles, left axis) and synaptic depression (open circles, right axis) from the data shown in $C_1$. ($C_3$) Linear regression of the EPSC steady state and back extrapolation (to time 0) from control and DKO synapses. ($D_1$–$D_3$) Average initial EPSC amplitude ($D_1$), RRP ($D_2$), and vesicle release probability ($D_3$) from control ($n$ = 9) and DKO neurons ($n$ = 11; $^*P < 0.05$, $^{**}P < 0.01$). (*E*) Representative EPSCs induced by paired-pulse stimuli at variable interpulse intervals from a control and a DKO neuron. (*Inset*) Synaptic responses at an expanded timescale. Note the strong facilitation at the DKO neuron. (*F*) Average paired-pulse ratios in control ($n$ = 16) and DKO ($n$ = 17) neurons show that the ratios from DKO neurons are higher at all time intervals tested.

sites 2 and 3 in its substrate synapsin 1. The inhibition also occurred and was much stronger, in the DKO neurons, consistent with an activated state of the kinase in these neurons (Fig. 8*B*).

Ant-AIP-II also slightly enhanced the synaptic depression observed at control synapses both at low- (1 Hz) and high (20 Hz)-frequency stimulation (Fig. 8 *C* and *D*). Importantly, it blocked the facilitation elicited by low-frequency stimulation at DKO synapses (Fig. 8*C*) and also strongly, although not completely, inhibited the facilitation produced by high-frequency stimulation (20 Hz) (Fig. 8*D*), thus implicating CaMKII signaling in these changes. However, because Ant-AIP-II has little effect on the early phase of synaptic facilitation elicited by high-frequency stimulation in DKO synapses (Fig. 8*D*), additional mechanisms should contribute to the synaptic facilitation.

## Discussion

This study demonstrates that the endocytic defect resulting from the combined absence of dynamin 1 and 3 has a major and unexpected impact on short-term synaptic plasticity at excitatory synapses. EPSCs evoked at DKO synapses are smaller due to the smaller RRP of synaptic vesicles. However, DKO synapses, instead of displaying an accelerated synaptic depression upon high-frequency AP stimulation, exhibit decreased release probability and strong facilitation, indicating the occurrence of mechanisms that preserve synaptic transmission in face of the dramatic reduction of the overall synaptic vesicle abundance. Surprisingly, given the overall reduction in the state of neuronal network activity of DKO cultures and the lower probability of release, these changes correlate with an increased activation state of CaMKII in DKO neurons and are reversed by inhibition of CaMKII. All these changes, including CaMKII activation, are to a large extent reversed by previous silencing of electrical activity, pointing to their dependence on a backup of endocytic vesicle traffic in stimulated nerve terminals. Collectively, our results demonstrate that the backup of synaptic vesicle recycling traffic produced by the lack of the two neuronal dynamins inhibits the probability of release, thus revealing an interesting aspect of the coupling between endocytosis and exocytosis at central excitatory synapses.

Despite the absence of the great majority of dynamin (the dynamin 2 isoform contributes minimally to the total level of dynamin in neurons) (35), synaptic transmission in DKO neurons still occurs and is strong enough to fire APs in postsynaptic neurons, as also shown by the occurrence of muscle movement in DKO mice in the minutes/hours after birth. However, the properties of synaptic transmission are different in DKO neuronal cultures.

The size of the RRP, a parameter that has a key role in defining synaptic strength and plasticity (4), is clearly decreased, as demonstrated both by electrophysiological data and by ultrastructural analyses of synaptic active zones. On the basis of these observations and the very strong decrease in the overall number of synaptic vesicles at DKO synapses, one would have expected faster depression and stronger vesicle depletion at mutant synapses upon prolonged stimulation. In striking contrast, two surprising results, opposite to these predictions, were obtained. First, synaptic facilitation in response to both low- and high-frequency AP stimulation was observed. Second, even at late

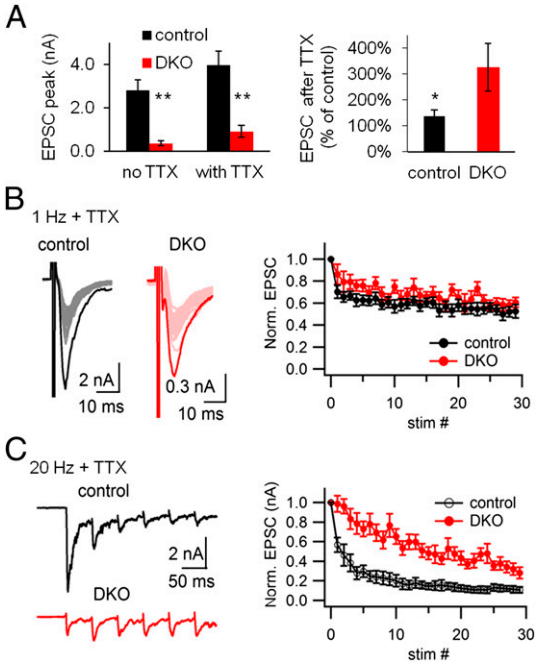


**Fig. 6.** Synaptic facilitation at DKO synapses is activity dependent and partially reversible. (*A*) EPSC amplitude increases after silencing spontaneous network activity with TTX in control and DKO neurons ($n = 14$ for control, $n = 10$ for DKO; $^*P < 0.05$, $^{**}P < 0.01$). (*B*) TTX exposure completely reversed the synaptic facilitation observed in DKO neuronal cultures upon stimulation at 1 HZ, so that a similar depression was observed in DKO and controls. Representative recording (*Left*) and normalized EPSCs (*Right*) from control ($n = 16$) and DKO neurons ($n = 14$) subjected to 1 Hz stimulation after overnight TTX treatment are shown. (*C*) TTX exposure also abolished the facilitation observed in DKO neurons upon high-frequency stimulation (20 Hz). In this case, a depression was observed in both DKO and controls, although this depression was smaller than controls. Representative recording (*Left*) and normalized EPSCs (*Right*) from control ($n = 13$) and DKO neurons ($n = 12$) subjected to 20 Hz stimulation after overnight TTX treatment are shown.

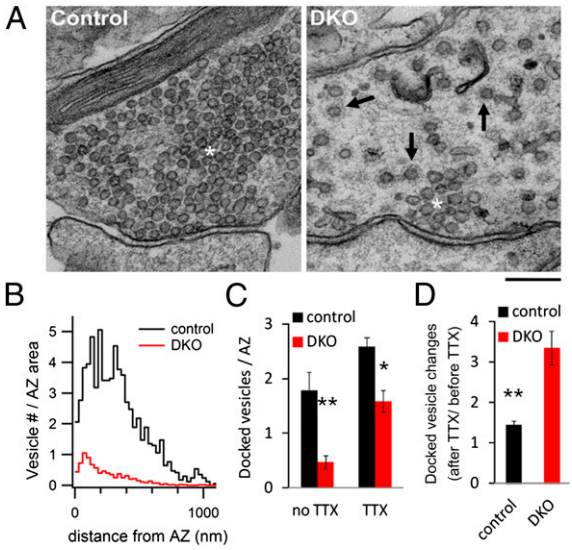


**Fig. 7.** Active zone ultrastructure and docked vesicles at DKO synapses. (*A*) Electron microscopy appearance of a control (*Left*) and a DKO (*Right*) synapse. Note in the DKO axon terminal the smaller synaptic vesicle cluster at the active zone of the synapse, which is surrounded by a large number of coated vesicular profiles (arrows), some of which have tubular necks in the plane of the section. As described previously (35), most clathrin-coated vesicular profiles are pits and not vesicles. White asterisks label the vesicle cluster in both micrographs. (Scale bar, 200 nm.) (*B*) Spatial distribution of synaptic vesicles around active zones in control ($n = 19$) and DKO synapses ($n = 80$). (*C*) Number of vesicles docked at the presynaptic plasma membrane of active zones before ($n = 19$, control; $n = 80$, DKO; $P < 0.01$) and after an overnight TTX treatment ($n = 86$, control; $n = 63$, DKO; $P < 0.01$). (*D*) Relative increase of the docked vesicle numbers per active zone after TTX treatment at control and DKO synapses. The data after TTX (shown in *C*) were normalized to the average number of docked vesicles before TTX was added. Note the stronger increase of the number of docked vesicles at DKO synapses.

stages of a stimulatory train, the normalized depression curve in DKO cultures never exceeded the depression observed in control neurons (although the two curves merged eventually). These results unmask a mechanism aimed at preserving the property to release neurotransmitters in the face of severely reduced vesicle availability in dynamin DKO synapses.

The facilitation observed in dynamin DKO mouse neurons is in contrast to the enhanced depression observed in mouse neurons that lack other abundant endocytic proteins and whose absence produces a delay in the clathrin-dependent reformation of synaptic vesicles, such as neurons from synaptojanin 1 KO mice and from endophilin triple-KO mice (16, 52, 74). The only mouse mutant synapses exhibiting a weaker depression than in control neurons are those lacking syndapin 1, a protein that has a major role in recruiting dynamin to synaptic membranes (75). A stronger depression than in controls was observed in flies and worms after genetic perturbation of endocytosis genes (other than *dynamin*, see below) that results in defects of synaptic vesicle recycling and smaller vesicle pools (10, 15, 18, 20, 21, 53, 76). Thus, it appears that a chronic defect in synaptic vesicle recycling is not sufficient to trigger facilitation and that some specific features of the endocytic block produced by dynamin are implicated. It will be of interest to determine whether the same phenomenon occurs at inhibitory synapses, because a previous study of the postsynaptic response at inhibitory synapses that lack dynamin 1 only did not reveal facilitation (9).

The facilitation observed here is also in contrast with the lack of facilitation observed at the neuromuscular junction of dynamin (*shibire*) mutants of *Drosophila* when stimulated at the restrictive temperature (18). However, there are some key differences in the experimental conditions under which these contrasting results were obtained. First, in our experiments we start from a baseline condition that is already highly compromised due to the smaller number of synaptic vesicles, the decreased size of the RRP, and the accumulation of endocytic intermediates. In fact, silencing of the cultures with an overnight exposure to TTX before our experiments, a condition that we have found to partially reverse many of the changes observed in DKO synapses relative to controls, abolished the facilitation, although a slower depression relative to controls was still observed. Second, the *Drosophila shibire* mutation is a dominant mutation (77, 78) whose effect on nerve terminal physiology can be accounted for not only by temperature-induced changes in dynamin itself, but also by the sequestration of dynamin binding partners, a scenario quite different from the near-lack of dynamin. The persistence of neurotransmitter release in the near absence of the overwhelming majority of dynamin is also in contrast to the block of action potential triggered endocytosis (79) and more pronounced depression (80) observed in neuronal cultures following exposure to dynasore, a compound that inhibits dynamin 1 and dynamin 2 (dynasore was not tested on dynamin 3, but the stronger similarity of dynamin 3 than of dynamin 2 to dynamin 1 makes it likely that dynasore also inhibits dynamin 3). Even in this case, the difference may be at least partially explained by the acute nature of experiments with dynasore. Moreover, the off-targets effect of dynasore should be considered because this drug was shown, for example, to have some effect on the dynamin-related protein 1 (DRP1) (81), to change $Ca^{2+}$ signaling (82, 83), and to affect actin dynamics (84).

One potential explanation for the functional changes reported here at DKO synapses is that they result from the dramatic backup of the endocytic traffic at the cell surface, where synaptic vesicle membranes (lipids and proteins) are stranded in clathrin-coated pits. The massive increase in the cell surface area and the corresponding structural changes of nerve terminals (35) may impact on the functional and biochemical parameters of the active zone and thus on release probability. Feedback mechanisms between membrane traffic and phosphorylation–dephosphorylation cascades may mediate the increase in CaMKII activity and synapsin phosphorylation (35). Supporting this possibility is the major reversal of facilitation and lowered release probability after TTX treatment, a treatment that silences the spontaneous network activity and results in the disappearance of the massive coated pit accumulation at DKO synapses. Another potential explanation is that the absence of the neuronal dynamins may result in a major perturbation of signaling. Dynamin binds many signaling proteins and may affect signaling via direct interactions with such proteins.

Whereas the precise mechanisms triggering facilitation remain to be elucidated, our results strongly suggest that the CaMKII activation via its phosphorylation at threonine 286 is an important mediator of these changes. Both the state of phosphorylation of synapsin 1 at CaMKII-dependent sites (sites 2 and 3) and autophosphorylation of βCaMKII at threonine 286 (85) are increased in DKO synapses. All these changes are reversed by inhibition of CaMKII activity or by TTX-dependent silencing of the cultures. It is interesting to note that synapsin 1 KO synapses have enhanced paired-pulse facilitation reminiscent of what we have observed in dynamin DKO synapses (86), raising the possibility that a chronic dissociation of synapsin 1 from the vesicles may play a role in such facilitation at DKO synapses. Whether the $Ca^{2+}$-dependent phosphatase calcineurin, which plays an important role in the $Ca^{2+}$-dependent dephosphorylation of several endocytic proteins including dynamin and directly binds the dynamin 1b splice variant (87, 88), is implicated in these changes remains an interesting question to address in future studies. Neither sites 1 and 2 of synapsin 1 nor threonine 286 of CaMKII are dephosphorylated by calcineurin, but the phosphorylation state of these sites could be controlled by dephosphorylation cascades triggered by calcineurin (89, 90).

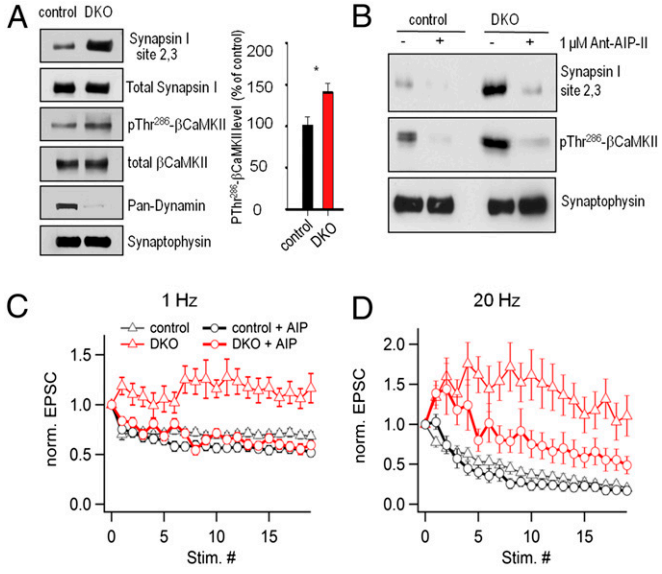


**Fig. 8.** Up-regulation of CaMKII activity contributes to facilitation at DKO synapses. (*A*) (*Left*) immunoblotting analysis revealing that levels of phospho-βCaMKII (threonine 286) and phospho-synapsin I (sites 2 and 3, serines 566 and 603) are increased in DKO neuronal cultures relative to control. Total levels of these proteins, as well as of synaptophysin, used as a loading control, are unchanged. The genotype of the DKO was confirmed by the pan-dynamin signal. (*Right*) Quantification (percentage of control) of the phospho-βCaMKII (threonine 286) signal in control and DKO cultures ($n = 4$). (*B*) Effect of the Ant-AIP-II peptide on the phosphorylation of βCaMKII (threonine 286) and synapsin I (sites 2 and 3). (*C* and *D*) Effect of the Ant-AIP-II peptide on short-term synaptic plasticity in response to low- (1 Hz) (*C*) and high (20 Hz) (*D*)-frequency stimulation in control ($n = 12$ and 11, respectively) and DKO synapses ($n = 10$ and 12, respectively).

Interestingly, syndapin 1, the only endocytic protein whose absence reduces, rather than enhances, synaptic depression (75), is the major protein whose interaction with dynamin is triggered by calcineurin-dependent phosphorylation (91).

In conclusion, our study demonstrates the occurrence of a feedback mechanism through which impaired dynamin-dependent endocytosis reduces the probability of release. This mechanism ensures persistence of neurosecretion even in the face of a profound reduction of synaptic vesicle number.

## Experimental Procedures

**Neuronal Culture.** Primary cortical neuron cultures were prepared from neonatal mouse brain as described previously (9). Dynamin 1 and 3 DKO (dynamin $1^{-/-}$; dynamin $3^{-/-}$) mice were generated from the mating of dynamin $1^{+/-}$; dynamin $3^{-/-}$ mice, and their littermates were used as controls to minimize variability. Such littermates controls (KO for dynamin 3 and either wild type or heterozygous for dynamin 1) did not differ in a significant way from wild-type newborn mice (35). In our experimental condition, the synaptic density between control and DKO cultures is comparable as demonstrated previously (35).

**Fluorescent $Ca^{2+}$ Imaging in Live Neurons.** Two different $Ca^{2+}$ imaging methods were used. $Ca^{2+}$ imaging to monitor spontaneous network activity (Fig. 1 and Fig. S1) was performed by Fura2-AM fluorescence (92). Imaging of presynaptic $Ca^{2+}$ dynamics was carried out by the fluorescent imaging of SyGCaMP3 that was expressed by adeno-associated virus-mediated gene transduction (Fig. S3).

**Patch-Clamp Recording.** Whole-cell patch clamp recordings were performed using the cultured neurons after 10–14 days in vitro differentiation (DIV) (35, 93). EPSCs were elicited by a local stimulation electrode connected with an isolated pulse stimulator. The holding potential was −70 mV unless otherwise noted and no liquid-junction potential correction was applied. Data were analyzed with Igor Pro (Wavemetrics). Cell-Permeable Autocamtide-2 Related Inhibitory Peptide II (Ant-AIP-II; Calbiochem) was added to the cultures (1 μM final concentration) 1 h before the recording and was continuously present during the recording.

**Biochemistry of Neuronal Cultures.** Determination of protein concentration, SDS/PAGE, and Western blotting were carried out by standard procedures (*SI Experimental Procedures*). For the analysis of the effect of Ant-AIP-II on protein phosphorylation, neuronal cultures were incubated with the drug as described above for electrophysiology.

**Electron Microscopy and Morphological Analysis.** Primary cortical cultures (18–22 DIV) were fixed with glutaraldehyde in sodium cacodylate buffer, post-fixed in $OsO_4/K_4Fe(CN)_6$, embedded in plastic, and stained with uranyl acetate following ultrathin sectioning (35). Images were taken with a Philips CM10 microscope and further analyzed with iTEM (Olympus) and Igor Pro software as described in *SI Experimental Procedures*.

**Statistics.** Unless otherwise specified, data were presented as mean ± SEM; statistical significance was determined using Student's *t* tests; $P < 0.05$ was taken as the level of significance; $*P < 0.05$, $**P < 0.01$.

For other details, see *SI Experimental Procedures*.

**ACKNOWLEDGMENTS.** We thank Frank Wilson, Lijuan Liu, and Louise Lucast for technical assistance. This work was supported in part by the G. Harold and Leila Y. Mathers Charitable Foundation, National Institutes of Health Grants R37NS036251 and DA018343, a National Alliance for Research on Schizophrenia and Depression distinguished Investigator Award (to P.D.C.), and a pilot grant from the Yale Diabetes Endocrinology Research Center (to X.L.).

1. Fioravante D, Regehr WG (2011) Short-term forms of presynaptic plasticity. *Curr Opin Neurobiol* 21:269–274.
2. Zucker RS, Regehr WG (2002) Short-term synaptic plasticity. *Annu Rev Physiol* 64: 355–405.
3. Dobrunz LE, Stevens CF (1997) Heterogeneity of release probability, facilitation, and depletion at central synapses. *Neuron* 18:995–1008.
4. Schneggenburger R, Sakaba T, Neher E (2002) Vesicle pools and short-term synaptic depression: Lessons from a large synapse. *Trends Neurosci* 25:206–212.
5. Dittman JS, Regehr WG (1998) Calcium dependence and recovery kinetics of presynaptic depression at the climbing fiber to Purkinje cell synapse. *J Neurosci* 18: 6147–6162.
6. Koenig JH, Ikeda K (2005) Relationship of the reserve vesicle population to synaptic depression in the tergotrochanteral and dorsal longitudinal muscles of Drosophila. *J Neurophysiol* 94:2111–2119.
7. Neher E, Sakaba T (2008) Multiple roles of calcium ions in the regulation of neurotransmitter release. *Neuron* 59:861–872.
8. Pan B, Zucker RS (2009) A general model of synaptic transmission and short-term plasticity. *Neuron* 62:539–554.
9. Ferguson SM, et al. (2007) A selective activity-dependent requirement for dynamin 1 in synaptic vesicle endocytosis. *Science* 316:570–574.
10. Dickman DK, Horne JA, Meinertzhagen IA, Schwarz TL (2005) A slowed classical pathway rather than kiss-and-run mediates endocytosis at synapses lacking synaptojanin and endophilin. *Cell* 123:521–533.
11. Wu LG, Ryan TA, Lagnado L (2007) Modes of vesicle retrieval at ribbon synapses, calyx-type synapses, and small central synapses. *J Neurosci* 27:11793–11802.
12. Murthy VN, De Camilli P (2003) Cell biology of the presynaptic terminal. *Annu Rev Neurosci* 26:701–728.
13. Royle SJ, Lagnado L (2010) Clathrin-mediated endocytosis at the synaptic terminal: Bridging the gap between physiology and molecules. *Traffic* 11:1489–1497.
14. Smith SM, Renden R, von Gersdorff H (2008) Synaptic vesicle endocytosis: Fast and slow modes of membrane retrieval. *Trends Neurosci* 31:559–568.
15. Verstreken P, et al. (2002) Endophilin mutations block clathrin-mediated endocytosis but not neurotransmitter release. *Cell* 109:101–112.
16. Cremona O, et al. (1999) Essential role of phosphoinositide metabolism in synaptic vesicle recycling. *Cell* 99:179–188.
17. Di Paolo G, et al. (2004) Impaired PtdIns(4,5)P2 synthesis in nerve terminals produces defects in synaptic vesicle trafficking. *Nature* 431:415–422.
18. Kawasaki F, Hazen M, Ordway RW (2000) Fast synaptic fatigue in shibire mutants reveals a rapid requirement for dynamin in synaptic vesicle membrane trafficking. *Nat Neurosci* 3:859–860.
19. Sato K, et al. (2009) Differential requirements for clathrin in receptor-mediated endocytosis and maintenance of synaptic vesicle pools. *Proc Natl Acad Sci USA* 106: 1139–1144.
20. Schuske KR, et al. (2003) Endophilin is required for synaptic vesicle endocytosis by localizing synaptojanin. *Neuron* 40:749–762.
21. Koh TW, Verstreken P, Bellen HJ (2004) Dap160/intersectin acts as a stabilizing scaffold required for synaptic development and vesicle endocytosis. *Neuron* 43: 193–205.
22. Shupliakov O, et al. (1997) Synaptic vesicle endocytosis impaired by disruption of dynamin-SH3 domain interactions. *Science* 276:259–263.
23. Gad H, et al. (2000) Fission and uncoating of synaptic clathrin-coated vesicles are perturbed by disruption of interactions with the SH3 domain of endophilin. *Neuron* 27:301–312.
24. Marie B, et al. (2004) Dap160/intersectin scaffolds the periactive zone to achieve high-fidelity endocytosis and normal synaptic growth. *Neuron* 43:207–219.
25. Hull C, von Gersdorff H (2004) Fast endocytosis is inhibited by GABA-mediated chloride influx at a presynaptic terminal. *Neuron* 44:469–482.
26. Xu J, et al. (2008) GTP-independent rapid and slow endocytosis at a central synapse. *Nat Neurosci* 11:45–53.
27. Neher E (2010) What is rate-limiting during sustained synaptic activity: Vesicle supply or the availability of release sites. *Front Synaptic Neurosci* 2:1–6.
28. Haucke V, Neher E, Sigrist SJ (2011) Protein scaffolds in the coupling of synaptic exocytosis and endocytosis. *Nat Rev Neurosci* 12:127–138.
29. Bai J, Hu Z, Dittman JS, Pym EC, Kaplan JM (2010) Endophilin functions as a membrane-bending molecule and is delivered to endocytic zones by exocytosis. *Cell* 143:430–441.
30. Poskanzer KE, Marek KW, Sweeney ST, Davis GW (2003) Synaptotagmin I is necessary for compensatory synaptic vesicle endocytosis in vivo. *Nature* 426:559–563.
31. Deák F, Schoch S, Liu X, Südhof TC, Kavalali ET (2004) Synaptobrevin is essential for fast synaptic-vesicle endocytosis. *Nat Cell Biol* 6:1102–1108.
32. Hui E, Johnson CP, Yao J, Dunning FM, Chapman ER (2009) Synaptotagmin-mediated bending of the target membrane is a critical step in Ca(2+)-regulated fusion. *Cell* 138: 709–721.
33. Nicholson-Tomishima K, Ryan TA (2004) Kinetic efficiency of endocytosis at mammalian CNS synapses requires synaptotagmin I. *Proc Natl Acad Sci USA* 101: 16648–16652.
34. Koo SJ, et al. (2011) SNARE motif-mediated sorting of synaptobrevin by the endocytic adaptors clathrin assembly lymphoid myeloid leukemia (CALM) and AP180 at synapses. *Proc Natl Acad Sci USA* 108:13540–13545.
35. Raimondi A, et al. (2011) Overlapping role of dynamin isoforms in synaptic vesicle endocytosis. *Neuron* 70:1100–1114.
36. Koenig JH, Ikeda K (1989) Disappearance and reformation of synaptic vesicle membrane upon transmitter release observed under reversible blockage of membrane retrieval. *J Neurosci* 9:3844–3860.
37. Hayashi M, et al. (2008) Cell- and stimulus-dependent heterogeneity of synaptic vesicle endocytic recycling mechanisms revealed by studies of dynamin 1-null neurons. *Proc Natl Acad Sci USA* 105:2175–2180.
38. Lou X, Paradise S, Ferguson SM, De Camilli P (2008) Selective saturation of slow endocytosis at a giant glutamatergic central synapse lacking dynamin 1. *Proc Natl Acad Sci USA* 105:17555–17560.

39. Ford MG, Jenni S, Nunnari J (2011) The crystal structure of dynamin. *Nature* 477: 561–566.
40. Faelber K, et al. (2011) Crystal structure of nucleotide-free dynamin. *Nature* 477: 556–560.
41. Clayton EL, et al. (2010) Dynamin I phosphorylation by GSK3 controls activity-dependent bulk endocytosis of synaptic vesicles. *Nat Neurosci* 13:845–851.
42. Takei K, McPherson PS, Schmid SL, De Camilli P (1995) Tubular membrane invaginations coated by dynamin rings are induced by GTP-gamma S in nerve terminals. *Nature* 374:186–190.
43. Roux A, Uyhazi K, Frost A, De Camilli P (2006) GTP-dependent twisting of dynamin implicates constriction and tension in membrane fission. *Nature* 441:528–531.
44. Chappie JS, et al. (2011) A pseudoatomic model of the dynamin polymer identifies a hydrolysis-dependent powerstroke. *Cell* 147:209–222.
45. Yamashita T, Hige T, Takahashi T (2005) Vesicle endocytosis requires dynamin-dependent GTP hydrolysis at a fast CNS synapse. *Science* 307:124–127.
46. Ferguson SM, De Camilli P (2012) Dynamin, a membrane-remodelling GTPase. *Nat Rev Mol Cell Biol*, 10.1038/nrm3266.
47. Ferguson SM, et al. (2009) Coordinated actions of actin and BAR proteins upstream of dynamin at endocytic clathrin-coated pits. *Dev Cell* 17:811–822.
48. Cook T, Mesa K, Urrutia R (1996) Three dynamin-encoding genes are differentially expressed in developing rat brain. *J Neurochem* 67:927–931.
49. Cao H, Garcia F, McNiven MA (1998) Differential distribution of dynamin isoforms in mammalian cells. *Mol Biol Cell* 9:2595–2609.
50. Murphy TH, Blatter LA, Wier WG, Baraban JM (1992) Spontaneous synchronous synaptic calcium transients in cultured cortical neurons. *J Neurosci* 12:4834–4845.
51. Cohen D, Segal M (2009) Homeostatic presynaptic suppression of neuronal network bursts. *J Neurophysiol* 101:2077–2088.
52. Milosevic I, et al. (2011) Recruitment of endophilin to clathrin-coated pit necks is required for efficient vesicle uncoating after fission. *Neuron* 72:587–601.
53. Verstreken P, et al. (2003) Synaptojanin is recruited by endophilin to promote synaptic vesicle uncoating. *Neuron* 40:733–748.
54. Malinow R, Malenka RC (2002) AMPA receptor trafficking and synaptic plasticity. *Annu Rev Neurosci* 25:103–126.
55. Kennedy MJ, Ehlers MD (2006) Organelles and trafficking machinery for postsynaptic plasticity. *Annu Rev Neurosci* 29:325–362.
56. Petrini EM, et al. (2009) Endocytic trafficking and recycling maintain a pool of mobile surface AMPA receptors required for synaptic potentiation. *Neuron* 63:92–105.
57. Lu J, et al. (2007) Postsynaptic positioning of endocytic zones and AMPA receptor cycling by physical coupling of dynamin-3 to Homer. *Neuron* 55:874–889.
58. Carroll RC, Beattie EC, von Zastrow M, Malenka RC (2001) Role of AMPA receptor endocytosis in synaptic plasticity. *Nat Rev Neurosci* 2:315–324.
59. Takahashi T, Svoboda K, Malinow R (2003) Experience strengthening transmission by driving AMPA receptors into synapses. *Science* 299:1585–1588.
60. Watt AJ, van Rossum MC, MacLeod KM, Nelson SB, Turrigiano GG (2000) Activity coregulates quantal AMPA and NMDA currents at neocortical synapses. *Neuron* 26: 659–670.
61. Poncer JC, Malinow R (2001) Postsynaptic conversion of silent synapses during LTP affects synaptic gain and transmission dynamics. *Nat Neurosci* 4:989–996.
62. Rosenmund C, Stevens CF (1996) Definition of the readily releasable pool of vesicles at hippocampal synapses. *Neuron* 16:1197–1207.
63. Lou X, Korogod N, Brose N, Schneggenburger R (2008) Phorbol esters modulate spontaneous and Ca2+-evoked transmitter release via acting on both Munc13 and protein kinase C. *J Neurosci* 28:8257–8267.
64. Schneggenburger R, Meyer AC, Neher E (1999) Released fraction and total size of a pool of immediately available transmitter quanta at a calyx synapse. *Neuron* 23: 399–409.
65. Wölfel M, Lou X, Schneggenburger R (2007) A mechanism intrinsic to the vesicle fusion machinery determines fast and slow transmitter release at a large CNS synapse. *J Neurosci* 27:3198–3210.
66. Tian L, et al. (2009) Imaging neural activity in worms, flies and mice with improved GCaMP calcium indicators. *Nat Methods* 6:875–881.
67. Zhao C, Dreosti E, Lagnado L (2011) Homeostatic synaptic plasticity through changes in presynaptic calcium influx. *J Neurosci* 31:7492–7496.
68. Dreosti E, Odermatt B, Dorostkar MM, Lagnado L (2009) A genetically encoded reporter of synaptic activity in vivo. *Nat Methods* 6:883–889.
69. Turrigiano GG (2008) The self-tuning neuron: Synaptic scaling of excitatory synapses. *Cell* 135:422–435.
70. Czernik AJ, Pang DT, Greengard P (1987) Amino acid sequences surrounding the cAMP-dependent and calcium/calmodulin-dependent phosphorylation sites in rat and bovine synapsin I. *Proc Natl Acad Sci USA* 84:7518–7522.
71. Chi P, Greengard P, Ryan TA (2001) Synapsin dispersion and reclustering during synaptic activity. *Nat Neurosci* 4:1187–1193.
72. Gardoni F, et al. (2009) Decreased NR2B subunit synaptic levels cause impaired long-term potentiation but not long-term depression. *J Neurosci* 29:669–677.
73. Jiang X, et al. (2008) Modulation of CaV2.1 channels by Ca2+/calmodulin-dependent protein kinase II bound to the C-terminal domain. *Proc Natl Acad Sci USA* 105: 341–346.
74. Luthi A, et al. (2001) Synaptojanin 1 contributes to maintaining the stability of GABAergic transmission in primary cultures of cortical neurons. *J Neurosci* 21: 9101–9111.
75. Koch D, et al. (2011) Proper synaptic vesicle formation and neuronal network activity critically rely on syndapin I. *EMBO J* 30:4955–4969.
76. Kawasaki F, et al. (2011) The DISABLED protein functions in CLATHRIN-mediated synaptic vesicle endocytosis and exoendocytic coupling at the active zone. *Proc Natl Acad Sci USA* 108:E222–E229.
77. Poodry CA, Hall L, Suzuki DT (1973) Developmental properties of Shibire: A pleiotropic mutation affecting larval and adult locomotion and development. *Dev Biol* 32:373–386.
78. Grigliatti TA, Hall L, Rosenbluth R, Suzuki DT (1973) Temperature-sensitive mutations in Drosophila melanogaster. XIV. A selection of immobile adults. *Mol Gen Genet* 120: 107–114.
79. Newton AJ, Kirchhausen T, Murthy VN (2006) Inhibition of dynamin completely blocks compensatory synaptic vesicle endocytosis. *Proc Natl Acad Sci USA* 103:17955–17960.
80. Chung C, Barylko B, Leitz J, Liu X, Kavalali ET (2010) Acute dynamin inhibition dissects synaptic vesicle recycling pathways that drive spontaneous and evoked neurotransmission. *J Neurosci* 30:1363–1376.
81. Macia E, et al. (2006) Dynasore, a cell-permeable inhibitor of dynamin. *Dev Cell* 10: 839–850.
82. Douthitt HL, Luo F, McCann SD, Meriney SD (2011) Dynasore, an inhibitor of dynamin, increases the probability of transmitter release. *Neuroscience* 172:187–195.
83. Tsai CC, et al. (2009) Dynasore inhibits rapid endocytosis in bovine chromaffin cells. *Am J Physiol Cell Physiol* 297:C397–C406.
84. Yamada H, et al. (2009) Dynasore, a dynamin inhibitor, suppresses lamellipodia formation and cancer cell invasion by destabilizing actin filaments. *Biochem Biophys Res Commun* 390:1142–1148.
85. Miller SG, Kennedy MB (1986) Regulation of brain type II Ca2+/calmodulin-dependent protein kinase by autophosphorylation: A Ca2+-triggered molecular switch. *Cell* 44: 861–870.
86. Rosahl TW, et al. (1995) Essential functions of synapsins I and II in synaptic vesicle regulation. *Nature* 375:488–493.
87. Xue J, et al. (2011) Calcineurin selectively docks with the dynamin Ixb splice variant to regulate activity-dependent bulk endocytosis. *J Biol Chem* 286:30295–30303.
88. Bodmer D, Ascaño M, Kuruvilla R (2011) Isoform-specific dephosphorylation of dynamin1 by calcineurin couples neurotrophin receptor endocytosis to axonal growth. *Neuron* 70:1085–1099.
89. Mulkey RM, Endo S, Shenolikar S, Malenka RC (1994) Involvement of a calcineurin/inhibitor-1 phosphatase cascade in hippocampal long-term depression. *Nature* 369: 486–488.
90. Jovanovic JN, et al. (2001) Opposing changes in phosphorylation of specific sites in synapsin I during Ca2+-dependent glutamate release in isolated nerve terminals. *J Neurosci* 21:7944–7953.
91. Anggono V, et al. (2006) Syndapin I is the phosphorylation-regulated dynamin I partner in synaptic vesicle endocytosis. *Nat Neurosci* 9:752–760.
92. Lou XL, et al. (2003) Na+ channel inactivation: A comparative study between pancreatic islet beta-cells and adrenal chromaffin cells in rat. *J Physiol* 548:191–202.
93. Lou X, Scheuss V, Schneggenburger R (2005) Allosteric modulation of the presynaptic Ca2+ sensor for vesicle fusion. *Nature* 435:497–501.